Structural Determinants of the Closed KCa3.1 Channel Pore in Relation to Channel Gating: Results from a Substituted Cysteine Accessibility Analysis

Hélène Klein, Line Garneau, Umberto Banderali, Manuel Simoes, Lucie Parent, and Rémy Sauvé

Department of Physiology, Membrane Protein Study Group, Faculty of Medicine, Université de Montréal, Montréal, Québec, Canada H3C 3J7

In this work we address the question of the KCa3.1 channel pore structure in the closed configuration in relation to the contribution of the C-terminal end of the S6 segments to the Ca^{2+}-dependent gating process. Our results based on SCAM (substituted cysteine accessibility method) experiments first demonstrate that the S6 transmembrane segment of the open KCa3.1 channel contains two distinct functional domains delimited by V282 with MTSEA and MTSET binding leading to a total channel inhibition at positions V275, T278, and V282 and to a steep channel activation at positions A283 and A286. The rates of modification by MTSEA (diameter 4.6 Å) of the 275C (central cavity) and 286C residues (S6 C-terminal end) for the closed channel configuration were found to differ by less than sevenfold, whereas experiments performed with the larger MTSET reagent (diameter 5.8 Å) resulted in modification rates 10^3–10^4 faster for cysteines at 286 compared with 275. Consistent with these results, the modification rates of the cavity lining 275C residue by MTSEA, Et-Hg^+, and Ag^+ appeared poorly state dependent, whereas modification rates by MTSET were 10^3 faster for the open than the closed configuration. A SCAM analysis of the channel inner vestibule in the closed state revealed in addition that cysteine residues at 286 were accessible to MTS reagents as large as MTS-PtrEA, a result supported by the observation that binding of MTSET to cysteines at positions 283 or 286 could neither sterically nor electrostatically block the access of MTSEA to the closed channel cavity (275C). It follows that the closed KCa3.1 structure can hardly be accountable by an inverted teepee-like structure as described for KcsA, but is better represented by a narrow passage centered at V282 (equivalent to V474 in Shaker) connecting the channel central cavity to the cytosolic medium. This passage would not be however restrictive to the diffusion of small reagents such as MTSEA, Et-Hg^+, and Ag^+, arguing against the C-terminal end of S6 forming an obstructive barrier to the diffusion of K^+ ions for the closed channel configuration.

The Journal of General Physiology

INTRODUCTION

Ca^{2+}-activated potassium channels (KCa) are present in most mammalian cell types, where their primary role is to establish a link between the various Ca^{2+}-based second messenger systems and the electrical properties of the cells. Three main classes of KCa to date have been identified based on their permeation properties and pharmacology (Vergara et al., 1998). They include the charybdotoxin- and iberiotoxin-sensitive KCa1.1 channels of large conductance (150–220 pS), the intermediate conductance (20–50 pS) KCa3.1 channels inhibited by clotrimazole (Rittenhouse et al., 1997) and TRAM34 (Wulff et al., 2001), and the apamine-sensitive and -insensitive SK channels of small conductance (KCa2.1, KCa2.2, and KCa2.3) (Kohler et al., 1996; Stocker, 2004). The KCa3.1 channel is a tetrameric protein with each subunit comprising 427 amino acids organized in six transmembrane segments S1–S6 with a pore motif between segments 5 and 6. In contrast to KCa1.1, the gating process of SK and KCa3.1 is voltage insensitive and the Ca^{2+} sensitivity is conferred by the Ca^{2+}-binding protein calmodulin (CaM), constitutively bound in the C terminus to each of the channel subunits in a 1:1 ratio (Khanna et al., 1999). CaM is also essential for the assembly and trafficking of the SK and KCa3.1 channel subunits (Joiner et al., 2001; Lee et al., 2003).

A 3D homology-based model of the pore-forming S6 transmembrane segment for the closed KCa3.1 configuration was proposed by our laboratory (Simoes et al., 2002) using the bacterial KcsA channel structure as template (Doyle et al., 1998). The resulting radial distribution of the α carbons for residues V275 to N292 along the S6 transmembrane segment is illustrated in Fig. 1 A. As seen, the V275, T278, and V282 residues are presented as lining the channel pore with V275 and T278

Correspondence to Rémy Sauvé: remy.sauve@umontreal.ca

Abbreviations used in this paper: MTS, methanethiosulfonate; MTSET, [2-(trimethylammonium)ethyl] methanethiosulfonate bromide; MTSEA, 2-aminoethyl methanethiosulfonate hydrobromide; MTS-PtrEA, [3-(triethylammonium)propyl] methanethiosulfonate; Et-Hg^+, ethylmercury; MTSACE, 2-(aminocarbonyl)ethyl methanethiosulfonate; MTSES, sodium (2-sulfanoethyl) methanethiosulfonate.

contributing to the formation of a central inner cavity ~10 Å wide. The V284 and V285 residues are predicted in turn to be oriented opposite to the pore lumen with the residue A286 at the C-terminal end of S6 pointing toward the pore central axis. More importantly, the diameter of the KCa3.1 conducting pathway is expected to vary along the channel central axis of diffusion with a minimum van der Waals diameter of 2.0 Å at the level of the V282 residue. It follows therefore that a pore structure for the closed KCa3.1 channel based on a KcsA template would be characterized by a bundle crossing region extending from V282 to A286 with the presence of a tight hydrophobic seal at the level of the V282 residue. Data supporting this model would strongly argue for a KCa3.1 activation gate located at the C-terminal end of the transmembrane S6 segments (for example see LeMasurier et al., 2001; Cordero-Morales et al., 2006).

In this work we address the question of the KCa3.1 channel pore structure in the closed configuration. Our results provide evidence that the pore structure of the closed KCa3.1 channel cannot be accounted for by the inverted teepee-like structure prevailing for KcsA, but rather support a model where the closed KCa3.1 is characterized by a narrow passage centered at V282 connecting the channel central cavity to the cytosolic medium. We conclude that the Ca^{2+}-dependent gating of KCa3.1 involves different sections of the S6 segment with the C-terminal end of S6 not constituting a hydrophobic seal capable to control K^+ ion flow.

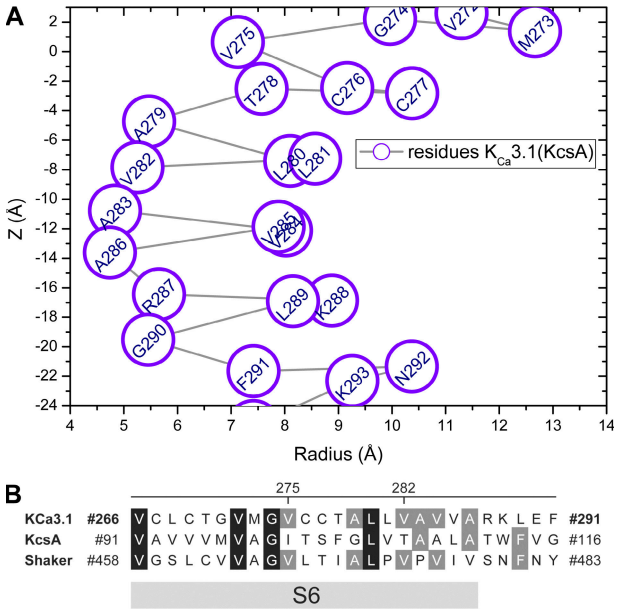

Figure 1. (A) Radial distribution of the α carbons for the residues V275 to N292 along the S6 transmembrane segment computed for the closed KCa3.1 structure generated using the KcsA channel as template. The Z axis refers to the pore central axis of diffusion with $z = 0$ centered at the level of the V275 residue. (B) Amino acid sequence alignment of the S6 transmembrane segment in KCa3.1, KcsA, and *Shaker* channels. The alignment was based on the highly conserved glycine hinge at position 274 in KCa3.1. Conserved residues are shaded in black (100%) and gray (67%), respectively. The S6 segment in KCa3.1 is presented as extending from V266 to A286.

MATERIALS AND METHODS

Cloning, Sequencing, and Site-directed Mutagenesis of the KCa3.1 Channel

KCa3.1 channel cDNA was obtained by RT-PCR from HeLa cells as previously described (Simoes et al., 2002). Site-directed mutagenesis was performed using the QuickChange site-directed mutagenesis kit (Stratagene). Point mutations were obtained using 25-mer mutated oligonucleotides with the wild-type KCa3.1 as template and confirmed by sequencing the entire coding region on both strands by automated fluorescently labeled sequencing (Bio S&T Inc.).

Oocytes

Mature oocytes (stage V or VI) were obtained from *Xenopus laevis* frogs anaesthetized with 3-aminobenzoic acid ethyl ester. The follicular layer was removed by incubating the oocytes in a Ca^{2+}-free Barth's solution containing collagenase (1.6 mg/ml; Sigma-Aldrich) for 45 min. Defolliculated oocytes were stored at 18°C in Barth's solution supplemented with 5% horse serum, 2.5 mM Na-pyruvate, 100 U/ml penicillin, 0.1 mg/ml kanamycin, and 0.1 mg/ml streptomycin. The composition of the Barth's solution was (in mM) 88 NaCl, 3 KCl, 0.82 $MgSO_4$, 0.41 $CaCl_2$, 0.33 $Ca(NO_3)_2$, and 5 HEPES (pH 7.6). Oocytes were patched 3–5 d after coinjection of 0.1–1 ng of the cDNA coding for KCa3.1 and 1 ng of cDNA coding for a green fluorescent protein that was used as a marker for nuclear injection.

Prior to patch clamping, defolliculated oocytes were bathed in a hyperosmotic solution containing (in mM) 250 KCl, 1 $MgSO_4$, 1 EGTA, 50 sucrose, and 10 HEPES buffered at pH 7.4 with KOH. The vitelline membrane was then peeled off using fine forceps, and the oocyte was transferred to a superfusion chamber for patch clamp measurements.

Solutions

The bath and patch pipette solutions contained (in mM) 200 K_2SO_4, 1.8 $MgCl_2$, 0.025 $CaCl_2$, 25 HEPES, buffered at pH 7.4 with KOH. The use of sulfate salts prevented excessive contaminations from endogenous Ca^{2+}-dependent chloride channels while enabling to chelate contaminant divalent cations such as Ba^{2+} (maximum free Ba^{2+} concentration: 0.5 nM in 200 mM K_2SO_4). Calcium-free solutions were prepared by adding 1 mM EGTA to 200 mM K_2SO_4 solutions without $CaCl_2$. In experiments where Et-Hg^+ was used as thiol modifying agent, the bath and patch pipette solution consisted of (in mM) 145 K-gluconate, 5 KCl, 2.5 $MgCl_2$, 0.1 EGTA, and 10 HEPES (pH adjusted to 7.4 with KOH). Ag^+ solutions were prepared by adding Ag_2SO_4 to Cl^--free 200 mM K_2SO_4 solutions that contained 60 mM EDTA without $CaCl_2$ and where $MgCl_2$ has been substituted by $MgSO_4$. The free Ag^+ concentration was calculated using the Eqcal software (Biosoft). Ca^{2+}-free 200 K_2SO_4 solutions at pH 6.5 and 5.5 were prepared by replacing HEPES by 25 mM MES plus KOH with either 10 mM EGTA (pH 5.5) or 2 mM EGTA (pH 6.5). For Ca^{2+}-free 200 K_2SO_4 solutions at pH 8.5, pH was adjusted with (in mM) 25 Tris plus HCl in the presence of 1 EGTA. 2-Aminoethyl methanethiosulfonate hydrobromide (MTSEA), sodium (2-sulfanoethyl) methanethiosulfonate (MTSES), [2-(trimethylammonium)ethyl] methanethiosulfonate bromide (MTSET), 2-(aminocarbonyl) ethyl methanethiosulfonate (MTSACE), and [3-(triethylammonium) propyl] methanethiosulfonate (MTS-PtrEA) (Toronto Research

Chemicals Inc.) were added directly into the bath solution just before application. Stock solution of MTSACE (500 mM) was prepared in DMSO. Bath solution changes were performed as described previously using a RSC-160 rapid solution changer system (BioLogic). The solution exchange time was estimated at 30 ms (Banderali et al., 2004).

Patch Clamp Recordings

Inside-out single channel recordings were performed using an Axopatch 200A amplifier (Axon Instruments, Inc.). Patch pipettes were pulled from borosilicate capillaries using a Narishige pipette puller (model PP-83) and used uncoated. The resistance of the patch electrodes ranged from 2 to 5 MΩ. Unless specified otherwise, the membrane potential is expressed as −Vp, where Vp is the pipette applied potential. Data acquisition was performed using a Digidata 1320A acquisition system (Axon Instruments, Inc.) at a sampling rate of 2.0 kHz and filtered at 500 Hz. Experiments were performed at room temperature (22°C).

Models To Estimate the Rate of Cysteine Modification by MTS Reagents

The binding of a MTS molecule to a cysteine residue at a channel site S_f can formally be expressed as (Wilson and Karlin, 1998)

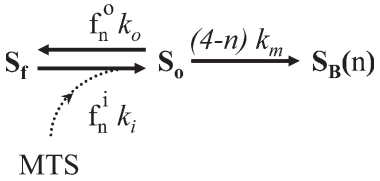

(SCHEME 1)

where n corresponds to the number of MTS-cysteine complexes formed $n \in \{0, 3\}$, k_i, the MTS entry rate to the cysteine binding site, k_o, the MTS exit rate from the cysteine binding site, k_m, the binding rate of the MTS to a single cysteine, and f_n^i, f_n^o, interaction parameters that account for the change in entry and exit rates when n MTS–cysteine complexes have already been formed. S_f represents the state of the cysteine binding site when not occupied by MTS, S_o, the site when occupied by MTS, and S_B, the site following the formation of a MTS–cysteine complex. The channel modification rate for a given MTS concentration ([MTS]) when n MTS–cysteine complexes have already been formed, K_n, is given by (see Appendix)

$$K_n \cong \frac{(4-n)k_i f_n^i [\mathrm{MTS}] k_m}{k_i f_n^i [\mathrm{MTS}] + k_o f_n^o + (4-n)k_m} \tag{1}$$

and the binding of four MTS reagents to a channel can now be modeled as a five state kinetic scheme with

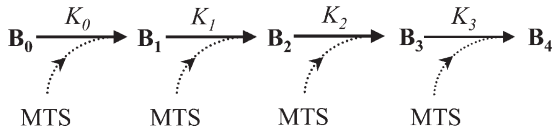

(SCHEME 2)

Because the proposed kinetic scheme with K_n given by Eq. 1 leads to a hardly tractable expression and to limit the number of adjustable parameters in our curve fitting procedure, we chose to analyze our experimental data according to two different kinetic models.

(1) Model I. In conditions where the exit rate from the binding site is much faster than the reaction with the cysteine ($k_m \ll k_o$), the channel modification rate at low MTS concentrations corresponds to $K_n = (4 - n)\, k_m k_i f_n [\mathrm{MTS}]/k_o$ (see Appendix) with $f_n = f_n^i / f_n^o$. The rates of transition K_n can now be expressed as $(4 - n)\, K_C f_n [\mathrm{MTS}]$ with the modification rate per cysteine K_C given by $K_C = k_m k_i / k_o$. The modification rate K_C does not in this case directly reflect the entry rate k_i, but also depends on the ratio k_m/k_o. The parameter f_n takes into account a possible negative cooperative effect due to the increase in free energy required to modify the $n + 1^{\mathrm{th}}$ cysteine residue when n MTS–cysteine complexes have been formed. Formally f_n can be expressed as $f_1{}^n \in \{1, 3\}$, with $f_0 = 1$.

(2) Model II. In conditions where the reaction rate with the cysteine is considered much faster than the entry and exit rates k_i and k_o ($k_m >> k_o + k_i[\mathrm{MTS}]$), the rates of transition K_n can be expressed as $K_n = k_i f_n^i [\mathrm{MTS}]$ (see Appendix) with f_n^i formally given by $f_n^i = (f_1^i)^n$ and $f_0^i = 1$. Assuming that there are no interactions between MTS molecules, $f_n^i = 1$ and K_n become independent of n with $K_n = k_i[\mathrm{MTS}]$. Under these conditions, modification rate measurements truly reflect the accessibility of the MTS reagents to the modification site independently of the reaction and exit rates k_m and k_o.

The time-dependent variation in current following the addition of MTS molecules can now be expressed as

$$I(t) = \sum_{n=0}^{4} P(B_n, t) \frac{N \Delta I}{1 + A\xi^n}(1 - ng), \tag{2}$$

where $P(B_n,t)$ is the probability for a channel to be in state B_n at time t, $N/(1 + A\xi^n)$ the mean number of open channels in state B_n, A the channel open/closed equilibrium constant before the addition of MTS, ΔI the unitary current amplitude, and g, the fractional decrease in unitary current following the binding of a single MTS molecule to the channel. With $f_n = 1$, Eq. 2 reduces for the Model I to the expression proposed by Flynn and Zagotta (2003) to determine the effects of MTS on CNG channel gating and permeation. The parameter ξ was introduced to account for the change in open probability when n MTS molecules are added to the channel structure. The expression $A\xi^n$ can formally be expressed as $\exp(-(\Delta G + n\Delta G_{\mathrm{MTS}})/\mathrm{KT})$ where ΔG is the difference in free energy between the channel closed and open configurations and ΔG_{MTS} the change in free energy between the closed and open configurations due to the binding of a single MTS reagent. If $\xi = 1$, the channel open probability becomes independent of the number of MTS–cysteine complexes formed, and Eq. 2 describes the time-dependent current inhibition resulting from the binding of MTS molecules to the channel. The time course of the current activation or inhibition was analyzed by adjusting the parameters N, f_0, A, ξ, and K_C (Model I) or N, A, ξ, f_0^i, and k_i (Model II) in Eq. 2 to best account for the experimental data. The parameters ΔI and g were directly derived from single channel recordings. In conditions where channel inhibition could be accounted for by a single exponential (V275C mutants in the closed state), the proposed five-state kinetic scheme reduces to a two-state model with the rate of channel inhibition given by

$$K_0 = \frac{4k_m[MTS]}{[MTS] + (k_o f_0^o + 4k_m)/k_i f_0^i}. \tag{3}$$

Rates of MTS-induced modification could under these conditions be directly computed as the ratio $K_0/[\mathrm{MTS}]$, where K_0 is the rate of channel block for a given MTS concentration. Curve fitting the experimental data to Eq. 2 and theoretical predictions based on Model I and Model II were performed using Mathematica 5.1 (Wolfram Research Inc.).

MTSEA Hydrolysis

Because the rate of MTSEA hydrolysis increases at alkaline pH (Karlin and Akabas, 1998), the time course of the MTSEA-induced current variations for experiments performed at pH 8.5 was

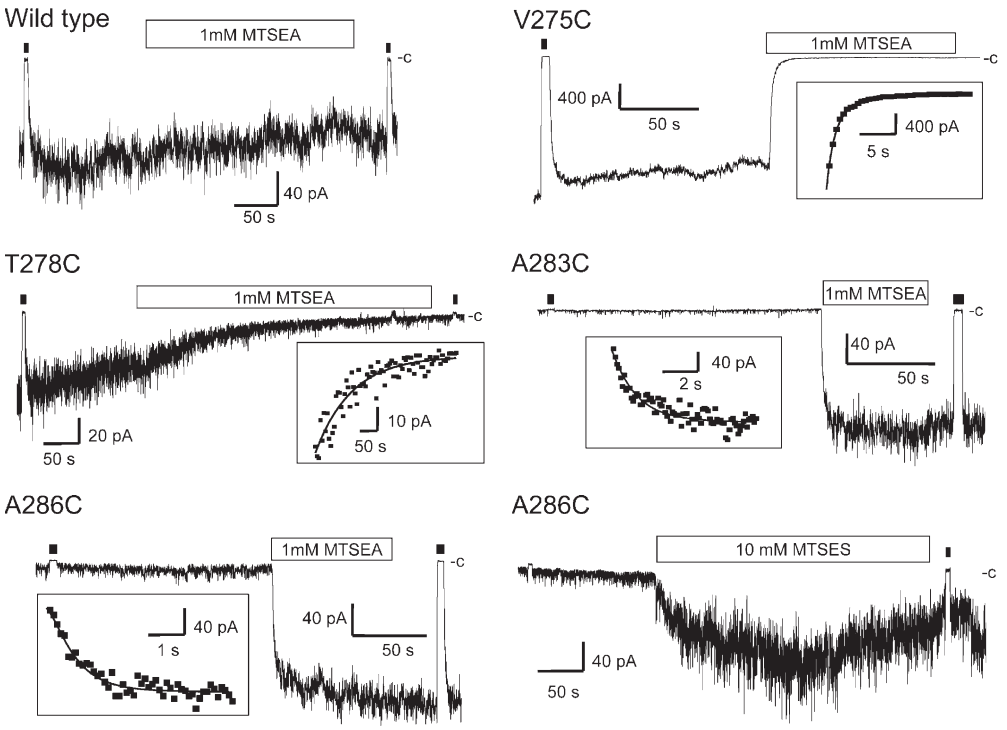

Figure 2. Inside-out current recordings obtained in 25 μM internal Ca^{2+} conditions illustrating the various effects of the positively charged MTSEA (1 mM) and negatively charged MTSES (10 mM) reagents on KCa3.1 channels where residues predicted to be facing the channel pore along the S6 transmembrane segment were substituted to cysteines. Perfusion with a zero Ca^{2+} solution is marked by a filled square. The symbol c refers to the current level for the closed KCa3.1 channel. There was no detectable effect of MTSEA applied for 4 min on KCa3.1 wild type. However, internal application of MTSEA caused a time-dependent inhibition of the V275C and T278C mutants while resulting in a robust current increase for cysteines engineered at positions 283 and 286. Also illustrated in insets are the theoretical curves computed by curve fitting to Eq. 2, the time-dependent current variation initiated following MTSEA application. Only 1 point out of 100 is presented for clarity. The time course of the current inhibition for the V275C and T278C mutants was best reproduced assuming the binding of two MTSEA molecules. In contrast, the results from the A283C and A286C are in accordance with the formation of four MTSEA–cysteine complexes, with the binding of each MTSEA leading to an increase of the channel open probability coupled to a 10–15% decrease of the channel unitary conductance per MTSEA. Current recordings performed in symmetrical K_2SO_4 conditions at −60 mV membrane potential.

corrected to account for the time-dependent changes in MTSEA concentration. The mean lifetime of MTSEA at pH 8.5 was estimated at 92 s based on absorbance measurements at 245 nm performed in 200 mM K_2SO_4 conditions.

Computer-based Homology Modeling

The closed KCa3.1 channel model structure was produced by automated homology modeling using Modeller v7.0 and involved the generation of 150 models using KcsA (PDB 1K4C) as template (Sali and Blundell, 1993). The model with the lowest objective function and the lowest RMS deviation between the template and the model was kept and used as model structure for the closed KCa3.1 channel. The overall structural quality of the generated models was evaluated by PROCHECK (Laskowski et al., 1993) and ProQ (Wallner and Elofsson, 2003).

Online Supplemental Materials

The PDB file generated by Modeller containing the atom coordinates of the best model obtained for the closed KCa3.1 has been included as online supplemental material (available at http://www.jgp.org/cgi/content/full/jgp.200609726/DC1).

RESULTS

Evidence for Two Functional Domains along S6

Fig. 2 presents typical macroscopic currents in response to channel modification by internal application of MTSEA for cysteine residues engineered at positions 275–287 along S6. MTSEA is a positively charged compound with dimensions corresponding to a cylinder 8.2 Å long with a diameter of 4.6 Å (space-filling estimation). The inside-out current recordings illustrated in Fig. 2 were performed in the presence of 25 μM Ca^{2+} and thus reflect the action of internal MTSEA on the open KCa3.1 channel (Po ranging from 0.2 to 0.4; see Banderali et al., 2004). The results in Fig. 2 confirm that the wild-type KCa3.1 is rather insensitive to MTSEA (1 mM), in accordance with the model proposed in Fig. 1 A where the C276 and C277 residues are oriented opposite to the pore lumen and thus poorly exposed to the water-filled conduction pathway. In contrast, a total and irreversible MTSEA-dependent current inhibition was recorded with the V275C and T278C mutants (Fig. 2) and with the V282C channel as well (not depicted), suggesting that the V275, T278, and V282 residues are accessible to water and oriented toward the channel pore. In addition, fitting the current traces obtained for the V275C, T278C, and V282C mutants to Eq. 2 revealed a time course for current inhibition characterized by a two exponential function and a minimal fractional decrease in unitary current per MTSEA of 80% (parameter $g = 0.8$ in Eq. 2). This analysis thus suggests that the binding of two MTSEA in the channel central cavity may be required for a total current inhibition, with the first MTSEA already accounting for 80% of the current

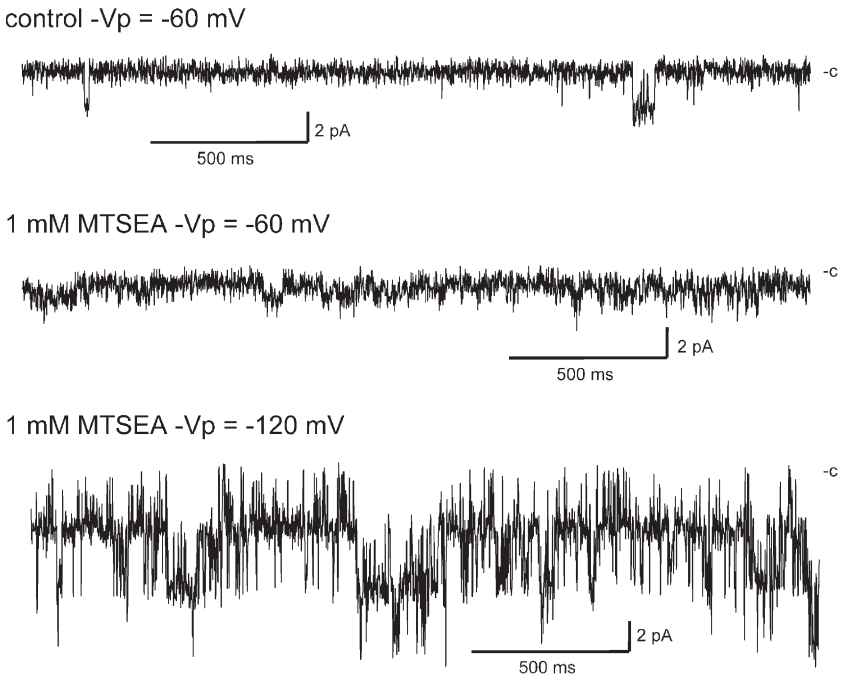

Figure 3. Example of single channel recording illustrating the stimulatory action of MTSEA on the 286C mutant. The amplitude of the current jumps recorded before MTSEA application was estimated at 2.4 pA at −60 mV membrane potential with a *Po* of 0.01 based on the entire recording. The unitary current amplitude following MTSEA binding to A286C decreased to 1 pA and 2.6 pA at −60 and −120 mV membrane potential, respectively, with a *Po* of 0.35 based on the entire recording. Recording obtained in symmetrical 200 K_2SO_4 conditions at saturating Ca^{2+} concentration (25 μM).

decrease. In contrast to the total current inhibition recorded with the V275C, T278C, and V282C mutants, the modification by MTSEA of cysteine residues engineered at positions 283 and 286 and to a lesser extent 285 (unpublished data) led to a robust current increase. Ca^{2+} dose–response measurements performed on the A286C mutant showed no change in the Ca^{2+} concentration for half activation compared with wild-type KCa3.1 ($[Ca^{2+}]_{1/2}$ = 1.2 μM) (Simoes et al., 2002), but the Ca^{2+} sensitivity of the A286C and A283C mutants activated by MTSET appeared slightly increased with a $[Ca^{2+}]_{1/2}$ estimated at 300 nM (unpublished data). The increase in channel activity observed following the binding of MTS reagents cannot therefore be ascribed to a change in Ca^{2+} sensitivity, as 25 μM Ca^{2+} constitutes a saturating Ca^{2+} concentration with and without MTS binding. Examples of the single channel current fluctuations illustrating the action of MTSEA on the A286C mutant are presented in Fig. 3. As seen, the binding of MTSEA to A286C resulted in a ≈50% decrease in unitary current amplitude accompanied by a strong increase in open probability (35-fold). These observations confirm the single-channel results on the MTSET-dependent activation of the A283C and A286C mutants reported in a previous work (Simoes et al., 2002). On the basis of these parameters, the time course of the current variations initiated by MTSEA for A286C and A283C channels was curve fitted to Eq. 2 using $g = 0.15$ with ξ ranging from 0.2 to 0.7. The current variations were best described by the successive binding of four MTSEA molecules to the channel, leading to either multiple exponential or sigmoid type variation in current amplitude as a function of time depending on the value of the parameter ξ. Altogether, these results indicate that the transmembrane S6 segment has two functional domains delimited by V282, a first domain extending from V275 to V282 constituting the channel central cavity and a second domain extending from A283 to A286 involved in the control of the channel open probability.

The Open Pore Structure as Revealed by MTSEA and MTSET

Fig. 4 summarizes the modification rates derived from Eq. 2 for cysteine residues engineered along S6 using either MTSEA or MTSET as modifying agents. These experiments were performed in the presence of 25 μM free Ca^{2+} to ensure that KCa3.1 channels were maximally activated. This figure clearly shows that MTSEA did not strongly discriminate between cysteines at 275 predicted to be lining the channel central cavity (Fig. 1 A), and cysteines engineered at the C-terminal end of S6 (A286) (Fig. 4 A). Notably, the slowest rates of modification were observed with the T278C and V282C mutants, respectively, indicating that these residues were less accessible than 275C to MTSEA modification. These conclusions remain valid whether the reaction rates K_n were computed according to Model I where $K_n = (4 - n)K_C[\text{MTS}]f_n$, with K_C the modification rate by cysteine or to Model II with $K_n = k_i f_n^i[MTS]$ (see Materials and methods). Because the mutations into cysteine of the residues at 280 and 281 yielded poorly functional channels, neither current inhibition nor current activation could be measured with cysteines engineered at these positions. Significantly more important variations in modification rates were obtained in experiments

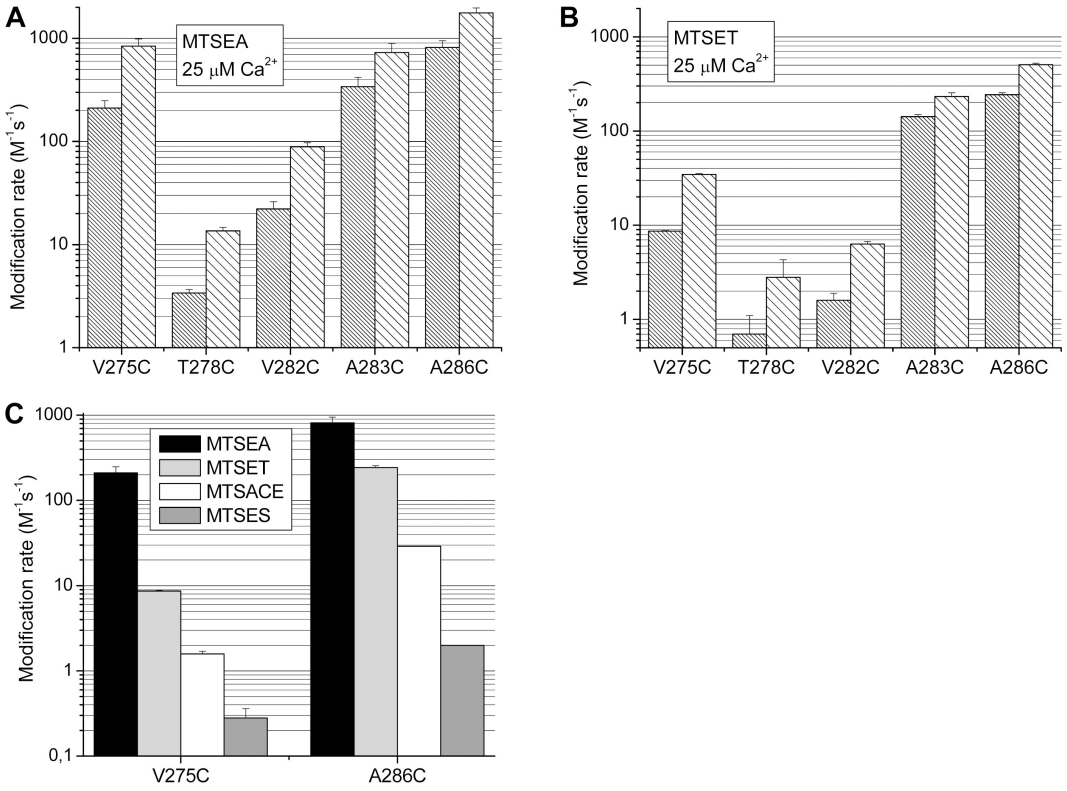

Figure 4. (A and B) Column graph representations of the modification rates measured in 25 μM Ca^{2+} conditions for residues along the S6 segment predicted to be facing the channel pore using MTSEA (A) and MTSET (B) as reagents. The rates of modification per cysteine K_C estimated using Model I are illustrated as dense pattern columns, whereas the modification rates k_i computed from Model II are shown as sparse pattern columns. In both cases the interaction parameters f_1 and f_1^i were set to 0.98. The modification rates were computed for each mutant channel by curve fitting to Eq. 2 the time-dependent current variation triggered following the internal addition of MTSEA or MTSET in 25 μM internal Ca^{2+}. The lowest rates of modification were obtained with the T278C and V282C mutants. (C) Column graph showing the modification rates measured for the V275C and A286C mutant channels using either a positively charged (MTSEA and MTSET), negatively charged (MTSES), or neutral (MTSACE) reagent. The modification rates were obtained by curve fitting to Eq. 2 the current variations induced by each MTS reagent. The modification rate K_C given by Model I were found to strongly depend on the charge of the MTS with faster rates of modification with the positively charged MTSEA and MTSET as compared with the neutral MTSACE or negatively charged MTSES.

performed using the larger MTSET reagent (space-filling diameter 5.8 Å, 10 Å long) (Fig. 4 B). There was a 28-fold decrease in modification rates by MTSET between 275C relative to 286C compared with a fourfold decrease with MTSEA. As observed with MTSEA, slower modification rates were obtained with cysteine residues at positions 278 and 282 compared with 275, suggesting again that these residues are less accessible to MTS modification than V275. Taken together, these observations indicate that the channel central cavity in the open state is readily accessible to MTSEA and MTSET. Experiments were next performed to determine if a local electrical potential within the pore could attract or repel MTS reagents according to their charge. The column graph presented in Fig. 4 C shows that the modification rates by the negatively charged MTSES reagent (space-filling diameter of 5.8 Å, 10 Å long) of cysteines at positions 275 and 286 are decreased 750-fold and 400-fold, respectively, relative to MTSEA. When compared with MTSET, the rates of modification by MTSES appeared 30-fold and 120-fold smaller for cysteines at positions 275 and 286, respectively. Finally, the rates of modification measured for cysteines at 275 were on the average six times smaller using the neutral MTSACE reagent (space filling diameter 6 Å and 10 Å long) compared with MTSET, although their dimensions are equivalent. Clearly the access of MTS reagents to the 275 and 286 residues for the open KCa3.1 strongly depends upon the presence of a local electrical potential that favors positively charged modifying agents.

Accessibility of Pore Residues in the Closed Conformation

A similar approach was used to probe the pore structure of the closed KCa3.1 channel. In these inside-out experiments, pulses of MTS reagents were applied for periods ranging from 0.5 to 5 s in zero internal Ca^{2+} conditions. The binding of the MTS reagent to the target cysteines was assayed by measuring the magnitude of the currents in 25 μM internal Ca^{2+} after each MTS pulse following the washout of the thiol modifying agent (see Fig. 5).

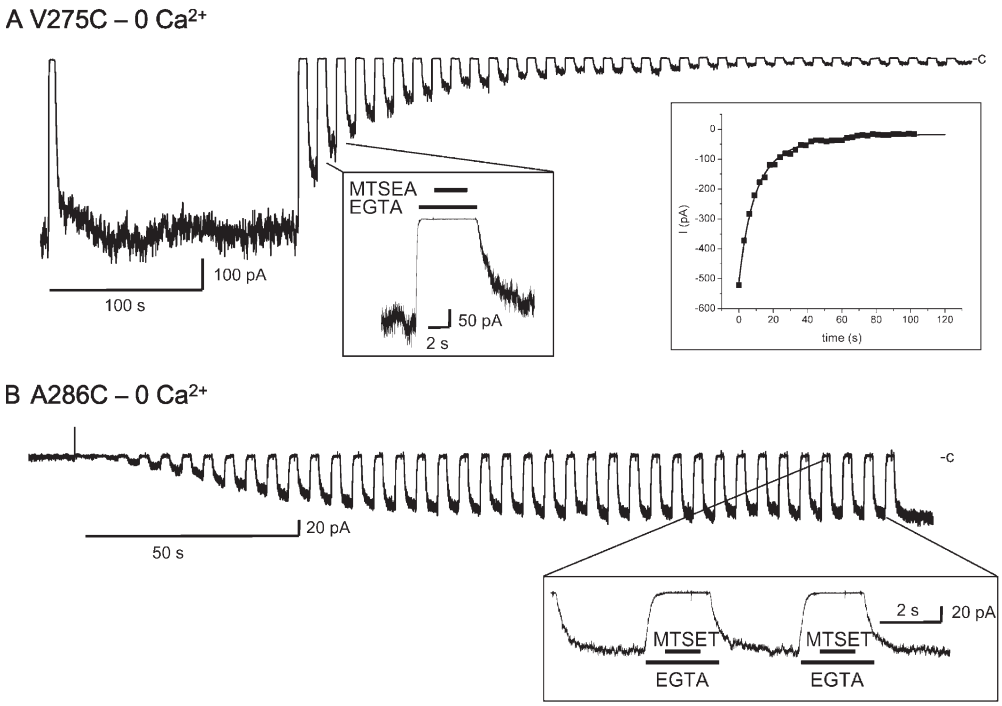

Figure 5. (A) Protocol used to measure the modification by MTSEA of a cysteine engineered in the channel central cavity (V275C) in zero (EGTA) internal Ca^{2+} conditions. MTSEA was applied for 3 s during 5.5-s pulses in zero internal Ca^{2+} conditions at a frequency of 0.1 Hz. The modification rates by MTSEA of the closed V275C mutant were estimated by fitting to Eq. 2 the time course of the test currents measured in 25 μM internal Ca^{2+} for each pulse following the washout of MTSEA (see inset). As illustrated, MTSEA could access the cysteine at position 275 in the channel central cavity with KCa3.1 in a closed configuration. (B) Channel activation induced by MTSET (1 mM)reacting with the A286C mutant in zero (EGTA) internal Ca^{2+} conditions. MTSET was applied for 1.0 s during a 2.0-s perfusion period with a Ca^{2+}-free solution. The time course of the current variation induced by MTSET was measured as described in A. This recording demonstrates that the cysteine substituting for the alanine at 286 reacted with MTSET in conditions where KCa3.1 was maintained in a closed state configuration. All recordings were obtained at $-Vp = -60$ mV in symmetrical 200 K_2SO_4 conditions. The symbol c refers to the current level for the closed KCa3.1 channel.

The action of MTSEA and MTSET on the closed V275C and A286C channels, respectively, is illustrated in Fig. 5. The inside-out recordings presented in this figure provide evidence that cysteine residues engineered at positions 275 and 286 are accessible to MTSEA and MTSET, respectively, in zero internal Ca^{2+} conditions. The modification rates measured in zero Ca^{2+} for cysteines substituting for S6 residues predicted on the basis of the KcsA structure to be facing the channel pore are summarized in Fig. 6 (A and B). The rates were computed according to Model I and Model II by fitting to Eq. 2 the time-dependent current variations resulting from the repetitive application of either MTSEA or MTSET. The overall profile presented in Fig. 6 A for MTSEA shows that the modification rate per cysteine K_C estimated from Model I varied from 480 ± 22 $M^{-1}s^{-1}$ ($N = 3$) for cysteines at the C-terminal end of S6 (286C) to 29 ± 3 $M^{-1}s^{-1}$ ($N = 7$) and 7 ± 3 $M^{-1}s^{-1}$ ($N = 2$) for cysteines at positions 275 and 278, respectively. In contrast, the modification rates estimated for the larger MTSET were reduced 10^4-fold for cysteines at 275 compared with cysteines at the cytoplasmic end of S6 (211 ± 25 $M^{-1}s^{-1}$, $N = 4$, for 286C). The access of MTS reagents to residues inside the channel central cavity for the closed KCa3.1 appears therefore to strongly depend upon the dimensions of the reagents comparatively to residues located down 282. This conclusion holds independently of the kinetic model used. Experiments performed using the T278C and V282C mutants led to no detectable MTSET-induced current modifications over a period of 5 min for the closed channel (Simoes et al., 2002).

How Does Channel Opening Affect the Channel Pore Structure ?

The results presented in Figs. 4 and 6 were also used to probe the conformational changes between the KCa3.1 pore structure in zero and saturating (25 μM) internal Ca^{2+}, respectively. Fig. 7 A summarizes the rates of modification by MTSEA and MTSET of cysteine residues substituting for amino acids predicted to be facing the pore for the KCa3.1 open and closed configurations. MTSEA was found to poorly discriminate between the channel open and closed conformations with modification rates for the V275C and A286C mutants, respectively, 7 and 1.7 times higher in 25 μM internal Ca^{2+} relative to zero internal Ca^{2+} conditions. A sevenfold difference in the V275C modification rate by MTSEA between the open and closed states reflects structural changes affecting the accessibility of residues inside the channel central cavity, but can hardly account for the gating of KCa3.1 by Ca^{2+}. Control experiments were also performed to determine to what extent the presence of two endogenous cysteines at positions 276 and 277 could contribute to the weak state dependence of the V275C accessibility to MTSEA. Experiments performed using the triple mutant V275C-C276G-C277S showed that the open/closed channel accessibility to MTSEA differs by ≈4-fold, indicating that our conclusion

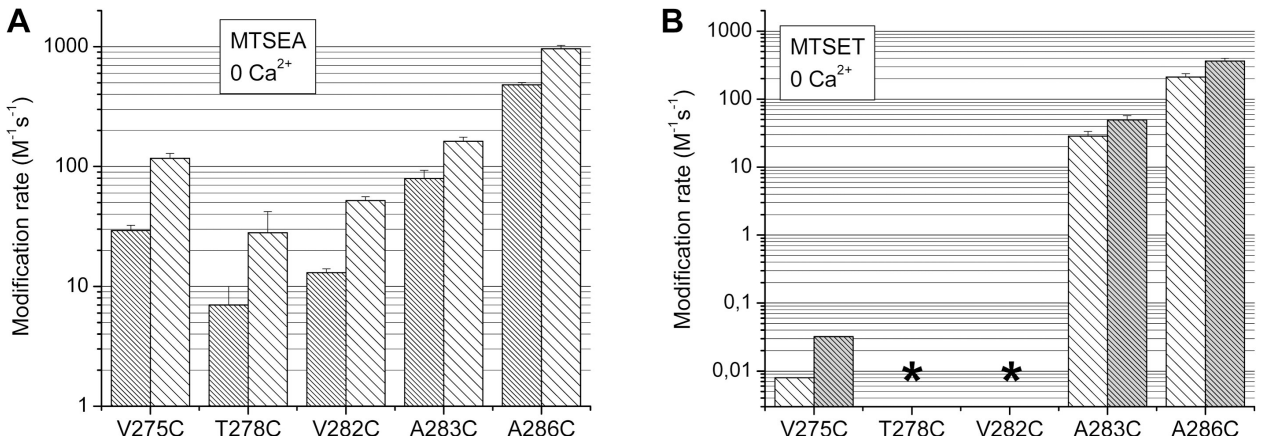

Figure 6. Column graph representations of the modification rates measured in zero Ca^{2+} conditions for residues along the S6 segment predicted to be facing the channel pore using MTSEA (A) and MTSET (B) as reagents. Dense pattern and sparse pattern columns are defined as described in Fig. 4. These results indicate that the modification rates measured with MTSEA varied by <10-fold (V275C relative to A286C) for residues located along the S6 segment, whereas a 10^4-fold decrease in modification rates was measured with MTSET for cysteines at 275C in the channel central cavity as compared with cysteines distal to V282 (positions 283–286). Stars refer to modification rates $<10^{-3}\ M^{-1}s^{-1}$.

on MTSEA discriminating weakly between the open and closed states truly reflects the accessibility of the cavity lining 275C residues. Fig. 7 A also indicates that the modification rates estimated for the T278C and V282C mutants is state independent, suggesting that the region distal to V282 is not obstructive to MTSEA diffusion for the open and closed configurations. In contrast, the modification rates measured with MTSET for cysteines at 275 was reduced at least 10^3-fold in zero Ca^{2+} as compared with rates measured in 25 μM Ca^{2+} conditions. This 10^3-fold variation is likely to represent a minimum value as V275C channels in zero Ca^{2+} were on the average inhibited by <20% after a 7-min exposure to MTSET (10 mM). The results presented in Fig. 7 A also indicate that the modification rates estimated for cysteines at positions 283 and 286 are poorly state dependent, confirming that the accessibility of these residues is not influenced by the conformational changes triggered by channel opening. Finally, the effect of the pore dimensions in the closed configuration on the accessibility to the 275C was further investigated using ethyl mercury (Et-Hg^+) and Ag^+ as probes. Et-Hg^+ is smaller than MTSEA with dimensions corresponding to a sphere of a 4.1 Å diameter (space-filling estimation). This molecule is closer to the dimensions of a dehydrated K^+ ion (2.66 Å diameter) while being more hydrophilic than MTSEA. With a diameter of 2.55 Å, Ag^+ is similar in size to a K^+ ion. Because experiments performed using Ag^+ as a probe required a strong buffering of the Ag^+ concentration with the Ca^{2+}-chelator EDTA, accessibility measurements could not be performed in this case for the open channel configuration. Examples of inside-out current recordings illustrating the respective action of Et-Hg^+ and Ag^+ (25 nM) on the V275C mutant are presented in Fig. 8. Both reagents caused a strong current inhibition in zero Ca^{2+} conditions, indicating that they could access the channel cavity with the channel in the closed state. The results of these experiments are shown in Fig. 7 B. The time course of the current inhibition induced by Et-Hg^+ and Ag^+ could be well fitted by a single exponential, so that the rates of modification were computed for a simple two state model using K_0 as described in Materials and methods. The modification rates measured with Et-Hg^+ for the closed and open configurations of the V275C mutant were found to be nearly identical with values of 5,000 ± 1,000 $s^{-1}M^{-1}$ ($n = 3$) and 4,000 ± 800 $s^{-1}M^{-1}$ ($n = 3$) in zero and 25 μM internal Ca^{2+}, respectively. A modification rate of 3.1 ± $0.6 \times 10^7\ s^{-1}M^{-1}$ ($n = 4$) was estimated for Ag^+ acting on the closed V275C channel. This value is less than 10 times smaller than the diffusion-limited rate expected for this ion ($\sim 10^8\ s^{-1}M^{-1}$; del Camino and Yellen, 2001). Taken together, these results support the proposal that small positively charged thiol-reactive reagents such as MTSEA, Et-Hg^+, and Ag^+ permeate through the water-filled channel pore of the closed KCa3.1 channel and have access to the cavity lining residue V275 in a state-independent manner.

Do Modification Rate Measurements Truly Reflect MTS Accessibility to the Binding Site ?

The expression described in Eq. 1 indicates that the global rate of modification K_n measured experimentally includes the rate of reaction k_m, the exit rate k_o, and the entry rate k_i. It follows that the rate measured experimentally cannot always be considered as an estimation of accessibility as it is not a direct evaluation of k_i, the entry rate of the MTS reagent to the binding site. Experiments were thus conducted where the accessibility parameter k_i was analyzed from the modification rates

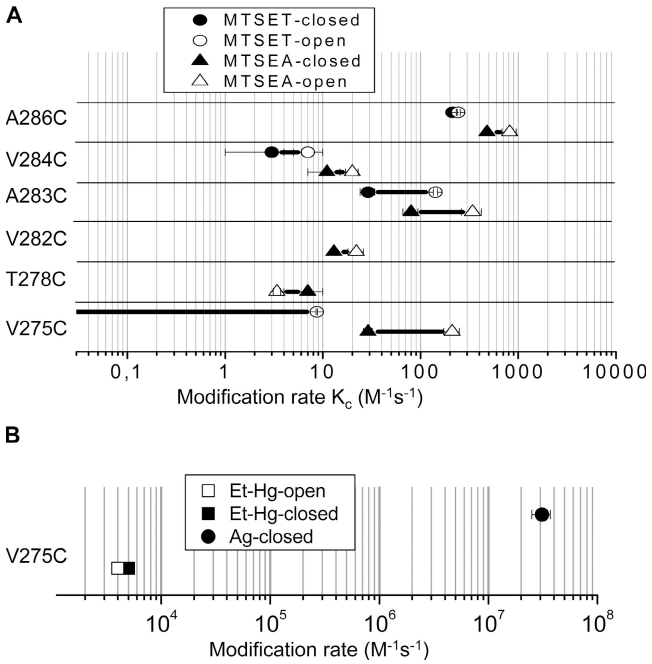

Figure 7. (A) Bar graph illustrating the state dependence of the modification rates measured for cysteine residues substituting for amino acids predicted to be facing the channel pore except for the V284 residue. The rates of modification per cysteine K_C obtained with MTSET (circles) in 25 μM (open symbols) and zero (filled symbols) internal Ca^{2+} conditions differed by 10^3-fold at the level of the cavity lining residue 275, in contrast to MTSEA (triangles) where modification rates differed by less than sevenfold. (B) Bar graph illustrating the state dependence of the modification rates by $Et\text{-}Hg^+$ (squares) and Ag^+ (circles) of the cysteine residues at position 275. The open/closed modification rates estimated using a simple two-state model with a transition rate given by K_0 were nearly identical. A modification rate of $3.1 \pm 0.6 \times 10^7$ $s^{-1}M^{-1}$ was obtained with Ag^+ for the closed V275C mutant. This value is close to the diffusion-limited modification rate expected for this ion, arguing for the C-terminal end of S6 being nonobstructive to Ag^+ diffusing inside the channel cavity. Taken together, these results suggest that the C-terminal end of S6 does not constitute the Ca^{2+}-dependent active gate of KCa3.1.

measured with MTSEA and MTSET on the V275C mutant. The validity of Eq. 1 in Materials and methods was first tested by estimating the modification rate K_0 as a function of the MTSEA concentration for the V275C mutant in 25 μM and zero internal Ca^{2+} conditions. As the current inhibition by MTSEA for the closed and open channel could be well approximated by a single exponential function, modification rates were thus computed using $g = 1$ in Eq. 2 with K_0 given by Eq. 3.

The results of these experiments are summarized in Fig. 9 A. The modification rates K_0 measured in zero internal Ca^{2+} show a strictly linear dependence as a function of [MTSEA] for concentrations ranging from 0.1 to 30 mM. This observation indicates that the cysteine binding site at 275 has a low affinity for MTSEA ($[MTSEA]_{1/2} >>$ 30 mM; see Appendix). The modification rates measured in 25 μM Ca^{2+} could be fitted to Eq. 1, leading to $k_m = 7.0\ s^{-1}$ and $[MTSEA]_{1/2} = 35$ mM. A $[MTSEA]_{1/2}$ value of ≈35 mM contrasts with an estimated $[MTSEA]_{1/2}$ value of 100 μM reported for the Kir 6.2 channel, suggesting important differences in MTSEA entry and exit rates between the two channels (Phillips et al., 2003). Again, as shown in Fig. 7 A, the modification by MTSEA of the cysteines at position 275 appeared poorly state dependent over the entire MTSEA concentration range considered. Clearly, experiments performed at 1–5 mM MTSEA are within the concentration range where K_n is directly proportional to [MTSEA], thus supporting our approach to measure modification rate using either Model I or II (see Materials and methods).

Next we took advantage of the fact that the reaction of MTS reagents with cysteine residues is strongly pH dependent, the reaction of MTS with protonated cysteine being 10^9-fold slower than the reaction with cysteine in a deprotonated form (Karlin and Akabas, 1998). The reaction rate k_m can thus formally be expressed as

$$k_m = \frac{k_m^0}{1+10^{pK_{a-cys}-pH}}, \tag{4}$$

where $k_m{}^0$ is the reaction rate for a totally deprotonated cysteine, and $pK_{a\text{-}cys}$ the expected pK_a value for cysteine ≈ 8.5. On the basis of the results presented in Fig. 9, equation K_n can now be rewritten as

$$K_n \cong \frac{(4-n)k_m^0 k_i}{(k_o f_n^o + (4-n)k_m^0)} \frac{1}{(1+10^{pK_{a-cys}-\log(\beta)-pH})}[\mathrm{MTSEA}], \tag{5}$$

where $\beta = 1 + (4-n)k_m^0 / k_o f_n^o$. Eq. 5 predicts that the titration of the modification rate K_n will approximate the titration curve of a cysteine residue only in conditions where $k_m{}^0 << k_o$. Fig. 10 illustrates the pH dependence of the modification rates measured for the V275C and A286C mutant channels in zero internal Ca^{2+} conditions. Because the KCa3.1 open probability was documented to be pH dependent, our measurements were performed in conditions where the channel was maintained in the closed configuration (Pedersen et al., 2000). The pH dependence obtained for the A286C mutant channel using MTSET (1 mM) as modifying agent is shown in Fig. 10 (curve A). The estimations obtained using Model I could be fitted to a titration curve with a pKa of 8.4, thus arguing for binding conditions such that $k_m{}^0 << k_o$. Curve A in Fig. 10 therefore supports a model where $K_n \approx nK_C[\mathrm{MTSEA}]$ with $K_C \approx k_i k_m / k_o$, indicating that experiments performed on the V286C mutant channel in zero internal Ca^{2+} largely underestimated the access rate k_i. Combining these observations and the results presented in Fig. 6 B, it is concluded that the MTSET access rate k_i for the closed A286C mutant channel should be >>200 $M^{-1}s^{-1}$, in agreement with a model for the closed KCa3.1 where the residues distal to V282 are readily accessible to

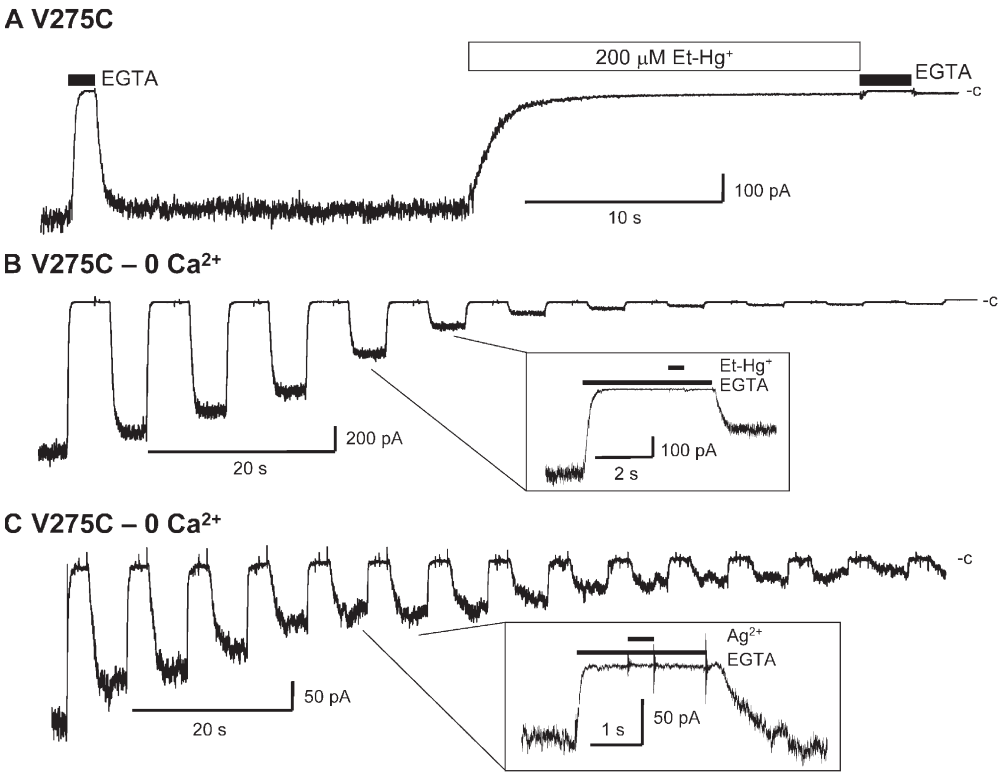

Figure 8. (A) Inside-out recording illustrating the inhibition of the V275C channel by Et-Hg$^+$ (200 μM) applied internally. The time course of the current inhibition was fitted to a single exponential function. (B) Protocol used to measure the modification by Et-Hg$^+$ of the closed V275C channel. Et-Hg$^+$ (120 μM) was applied for 0.5 s during 5-s pulses in zero internal Ca^{2+} conditions at a frequency of 0.12 Hz. The modification rates by Et-Hg$^+$ of the closed V275C mutant were estimated by fitting to a single exponential function the time course of the test currents measured in 25 μM internal Ca^{2+} for each pulse following the washout of Et-Hg$^+$ (see inset). The time course of the current inhibition was identical for the open and closed state. (C) Perfusion protocol as described in B with Ag$^+$ (25 nM) as modifying agent. These experiments required substantial buffering of the Ag$^+$ concentration (60 mM EDTA) for reproducibility and stability, thus limiting the use of Ag$^+$ to the closed configuration only as a μM concentration of free Ca^{2+} would have required to reduce the buffering of Ag$^+$. These experiments confirmed that Ag$^+$ could access the channel central cavity with the channel closed. Current recordings performed in symmetrical K_2SO_4 conditions at $-V_p = -60$ mV membrane potential.

MTSET. Curve A in Fig. 10 confirmed in addition that the observed pH dependence of the modification rate K_n truly reflects an effect on the reaction rate k_m between cysteines and MTS (Eq. 5), with little or no modulation of the entry and exit rates k_i and k_o. This conclusion is important as MTSET is expected to remain fully charged over the pH range 5.5–8.5 in contrast to MTSEA, which has been reported to be partially deprotonated at neutral pH (4%) with a pKa > 8.5 (Pascual and Karlin, 1998). Furthermore the pH dependence of the MTSET on V286C argues against a local pH value at 286 that would differ significantly from the bulk medium. The pH dependence measured with MTSEA acting on the A286C mutant (Fig. 10, curve D) in zero Ca^{2+} led to a pKa ≈ 6.1, arguing for $k_m^0/k_o >> 1$ (see Eq. 5) so that $K_n \approx k_i$[MTSEA]. Under these conditions, the results in Fig. 6 for MTSEA acting on A286C lead to $k_i = 960 \pm 63$ M^{-1}s^{-1} ($N = 3$). Finally, the pH dependence of the modification rate measured for MTSEA acting on the V275C mutant is shown in Fig. 10 curve B. Because the time course of the current inhibition for the closed V275C could be well fitted by a single exponential, the modification rates were computed from K_0 as discussed previously. The data points were fitted to a titration curve with a pKa of 7.8. According to Eq. 5 with $n = 0$, such a behavior would be indicative of a ratio $k_m/k_o \approx 0.07$ at pH 7.4 (Eq. 5). As $K_0 = 0.112$ s^{-1} for [MTSEA] = 1 mM (Fig. 9) at pH 7.4, Eq. 5 leads to $k_i \approx 480$ M^{-1}s^{-1}. This analysis of the MTSEA entry rate confirms that the cavity lining residues in the closed KCa3.1 channel are nearly as accessible to MTSEA as the residues located at the C-terminal end of S6.

Are MTSEA and K$^+$ Ions Using the Same Diffusion Pathway?

The results obtained with MTSEA suggest that molecules of 4.6 Å in diameter can access the channel cavity in the closed configuration. This is clearly not supported by a model of the closed KCa3.1 based on the KcsA structure. However, with a pKa > 8.5, 6% of the MTSEA molecules are neutral at pH 7.4 and can possibly access cysteines at 275 by diffusing through the lipid phase. A series of experiments was thus performed in which the modification rate of V275C by MTSEA was measured in zero and 25 μM Ca^{2+} conditions in the presence of the quaternary ammonium ion TBA in the channel central cavity. TBA applied internally has been documented to cause a total block of the V275C channel with half inhibition at 20 μM (Banderali et al., 2004), and the presence of positively charged TBA in the channel cavity should affect the time course of the MTSEA action if MTSEA diffuses in a protonated form. Examples of inside-out recordings obtained in 1 mM TBA conditions are presented in Fig. 11 A. Our results indicate that the presence of TBA decreased the MTSEA modification rates of the V275C

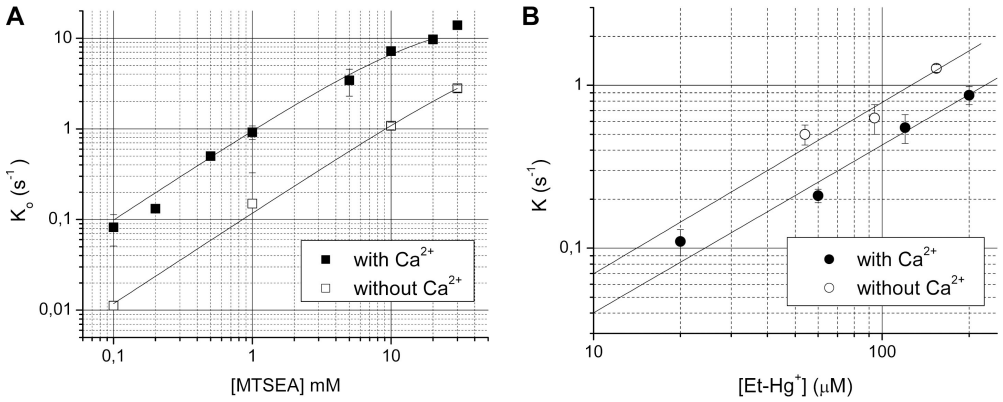

Figure 9. (A) Dose–response curves of the V275C inhibition rate K_0 as a function of the MTSEA concentration measured either in 25 μM (filled squares) or zero (empty squares) internal Ca^{2+} conditions. The modification rates were computed by fitting to a single exponential function the time course of the current inhibition induced by MTSEA using Eq. 2 with $g = 1$ and K_0 given by Eq. 3. The rates of modification obtained in zero internal Ca^{2+} were proportional to [MTSEA] for concentrations ranging from 0.1 to 30 mM, indicating a $[MTSEA]_{1/2} >> 30$ mM. The rates of modification measured in 25 μM Ca^{2+} conditions could be fitted to Eq. 1, leading to $k_m = 7\ s^{-1}$ and $[MTSEA]_{1/2} = 35$ mM. These results support an analysis of the modification rates K_n based on Eq. 1. In addition, the requirement in Model I and Model II of K_n being directly proportional to [MTS] is demonstrated to be valid for [MTSEA] < 5 mM. (B) Dose–response curves of the V275C modification rate measured either in 25 μM (filled circles) or zero (empty circles) internal Ca^{2+} conditions using Et-Hg^+ as thiol modifying agent. The data points obtained with Et-Hg^+ could be fitted to a linear equation for concentrations ranging from 20 to 200 μM. Slightly higher modification rates were measured in zero than 25 μM internal Ca^{2+} over the entire concentration range considered.

mutant computed for K_0 from 840 ± 136 $M^{-1}s^{-1}$ ($N = 7$) in zero TBA to 48 ± 8 $M^{-1}s^{-1}$ ($N = 2$) in 1 mM TBA for the open channel, and from 112 ± 12 $M^{-1}s^{-1}$ ($N = 7$) in the absence of TBA to 40 ± 4 $M^{-1}s^{-1}$ ($N = 4$) with TBA for the closed channel configuration. Our results thus indicate that MTSEA was sensitive to the presence of TBA in the channel cavity when the channel was maintained in a closed state. More importantly, the rates of modification were identical for the open and closed configurations in the presence of TBA. In conditions where the rate of reaction k_m with TBA becomes rate limiting, so that $K_0 \approx 4k_ik_m[\text{MTSEA}]/k_o$, this observation would be indicative of a ratio k_i/k_o identical for the open and closed state, arguing for the charged form of MTSEA being in equilibrium between the bulk medium and the central cavity when the channel is closed. If alternatively the presence of TBA leads to $k_m >> k_o$, so that $K_0 \approx k_i[\text{MTSEA}]$, our results would be indicative of TBA limiting the entry rate k_i, independently of the channel state, thus supporting the proposal that MTSEA accesses the 275C residues for the closed channel in a charged form. This proposal is also in agreement with the results presented in curve C (empty squares) of Fig. 10 on the pH dependence of the modification rate by MTSEA of the closed V275C mutant with TBA in the channel central cavity. The resulting titration curve led to a pKa of 6.9. As the modification rate K_0 = 0.040 s^{-1} for 1 mM [MTSEA] in the presence of TBA, Eq. 5 leads to $k_i \approx 54\ M^{-1}s^{-1}$. This analysis indicates that the presence of TBA caused a ≈9-fold decrease of the MTSEA entry rate, thus supporting the proposal that MTSEA accesses the closed channel cavity in a charged form. In addition, Eq. 5 predicts that for low MTSEA concentrations, the pH dependence of the MTSEA modification rate in conditions where only the neutral form of MTSEA has access to the 275C residue is given by

$$K_0 \cong \left(\frac{4k_m^0 k_i}{(k_o f_n^o + 4k_m^0)}\right)\left(\frac{1}{1+10^{pK_{a-cys}-\log(\beta)-pH}}\right)\frac{[MTSEA]_{total}}{1+10^{pKmtsea-pH}}, \quad (6)$$

where pKmtsea ≈ 8.5 (Karlin and Akabas, 1998), $[\text{MTSEA}]_{\text{total}}$ the total MTSEA concentration in the internal solution, and pKa-cys the pKa of the target cysteine residue (8.5). This expression predicts that the pH dependence of K_0 should essentially reflect the titration curve of MTSEA with a pKa value ≈ 8.5 independently of the parameter β. The titration curves presented in Fig. 10 for the V275C mutant should have therefore been identical with a pKa close to 8.5. This is not in agreement with our experimental observations as we found a pKa of 7.8 in the absence (Fig. 10, curve B) and 6.9 in the presence (Fig. 10, curve C) of TBA for the modification rate by MTSEA of 275C. The presence of TBA is not expected to affect the pKa of MTSEA, indicating that the observed variation of modification rates as a function of pH are not related to the protonation state of MTSEA. Our results do not therefore support the proposal of MTSEA diffusing in a neutral form to the channel cavity. Finally, because MTSEA was documented to be membrane permeant and to cause transmembrane cysteine modification (Holmgren et al., 1996; Karlin and Akabas, 1998), control experiments were performed in which the modification rate of the V275C mutant was measured in zero Ca^{2+} conditions with 5 mM cysteine added to the pipette solution. There was no effect due to the presence of cysteine in the patch electrode on the modification rate of the V275C mutant by MTSEA (unpublished data), ruling out a potential contribution of a trans-inhibition coming from the diffusion of MTSEA through the membrane.

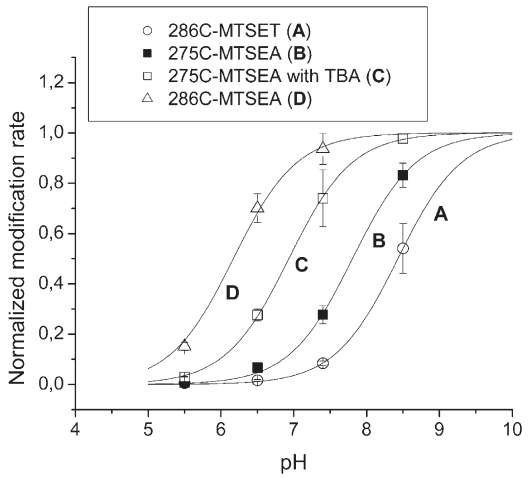

Figure 10. pH dependence of the modification rates measured for the V275C and A286C channels in zero internal Ca^{2+} conditions. Curve A (empty circles) shows the pH dependence obtained for the A286C mutant channel using MTSET (1 mM) as modifying agent. The data points (K_C from Model I) could be fitted to a titration curve with a pKa of 8.4, close to the pKa predicted for the protonation of a cysteine residue (8.5). This result confirms that the observed pH dependence of the modification rates K_n (Eq. 5) can be interpreted in terms of an effect on the reaction rate k_m (Eq. 4), with little or no modulation of the entry and exit rates k_i and k_o. Curve B (filled squares) shows the pH dependence of the modification rate measured for MTSEA acting on the V275C mutant in zero Ca^{2+}. The data points were obtained by curve fitting to a single exponential the time course of the current inhibition induced by MTSEA (K_0). The resulting curve was fitted to a titration curve with a pKa of 7.8 for a $k_m/k_o \approx 0.07$ at pH 7.4 . With $K_0 = 0.112\ s^{-1}$ at 1 mM MTSEA Eq. 5 leads to an entry rate $k_i = 480\ M^{-1}s^{-1}$. Curve C (empty squares) presents the pH dependence of the modification rate by MTSEA determined for the closed V275C mutant with TBA in the channel central cavity. The resulting titration curve led to a pKa of 6.9. As the modification rate $K_0 = 0.040\ s^{-1}$ for 1 mM [MTSEA], Eq. 5 leads to $k_i = 54\ M^{-1}s^{-1}$. Curve D (empty triangles) illustrates the pH dependence of the modification rate by MTSEA measured for the A286C mutant in zero Ca^{2+}. The titration curve was computed assuming a pKa $\approx$ 6.3 for a ratio $k_m^0/k_o >> 1$. k_i can then be directly estimated from K_n (Model II in Materials and methods) with $k_i = 961 \pm 63$ ($n = 3$) $M^{-1}s^{-1}$.

Can the Structure of the Closed KCa3.1 Channel distal to V282 be Represented by KcsA ?

The results obtained with MTSET on A283C and A286C mutants indicate that cysteines at 283 and 286 were accessible to MTSET in the closed channel configuration. The radial distribution of the α carbons for residues V275 to N292 presented in Fig. 1 A suggests however that A283 and A286 should participate in the formation of a bundle crossing region. Experiments were thus performed to investigate the topology of the pore region distal to V282 for the closed KCa3.1. In a first series of experiments, the accessibility of the 286C residue to the large MTS reagent MTS-PtrEA (space filling diameter of 9.5 and 12 Å long) was tested in zero Ca^{2+} conditions. The current recording presented in Fig. 11 B clearly shows that MTS-PtrEA could access the 286C residue with the channel in the closed configuration as the subsequent addition of Ca^{2+} revealed a strong channel activation as observed with MTSEA and MTSET. In a second series of experiments we took advantage of the fact that MTSET–cysteine complexes can be formed at positions 283 and 286 in zero internal Ca^{2+}, thus adding one to four positively charged residues within the channel inner vestibule. On the basis of the model presented in Fig. 1 A, the addition of positively charged residues at position 283 or 286 is expected to decrease the entry rate of MTSEA within the channel cavity in zero internal Ca^{2+} conditions and affect the modification rate of the cysteine residues engineered at V275. The experimental protocol used for measuring the rates of modification for the V275C-A283C and V275C-A286C double mutant channels is presented in Fig. 11 C. The time course of the current inhibition could be fitted by a single exponential so that the modification rates were estimated directly from K_0. The modification rates of 275C by MTSEA measured with MTSET–cysteine complexes at position 286 and 283 were estimated at 168 ± 8 $M^{-1}s^{-1}$ ($N = 3$) and 104 ± 4 $M^{-1}s^{-1}$ ($N = 3$), respectively, compared with 112 ± 12 $M^{-1}s^{-1}$ ($N = 7$) for the V275C simple mutant. The presence of positively charged residues within the channel inner vestibule for the closed KCa3.1 failed therefore to decrease the accessibility of MTSEA to cysteine residues located inside the channel central cavity. Finally, the KcsA-based structure predicted for the closed KCa3.1 illustrated in Fig. 12 A shows that the channel inner vestibule contains a double ring of histidine residues at positions 297 and 299. An additional histidine ring is also located at the level of the A286 residue coming from the four histidines in S5 at position 203. Because histidine residues are expected to be ~90% protonated at pH 5.5, substituting histidine to alanine under these conditions should cause the neutralization of ≈11 equivalent positive charges in the channel inner vestibule. The results presented in Fig. 12 B on the modification rates estimated at pH 5.5 for the triple V275C-H297A-H299A and quadruple V275C-H297A-H299A-H203A mutant channels provide evidence that the neutralization of ≈11 equivalent positive charges at the inner entrance of the KCa3.1 does not affect the cysteine accessibility of MTSEA to 275C in the closed channel configuration.

DISCUSSION

Two main conclusions follow from the observations reported in this work. First the S6 segment of the KCa3.1 channel contains two distinct functional domains delimited by the V282 residue with MTSEA and MTSET binding leading to a total channel inhibition for residues V275–V282 (V275, T278, and V282) and to a steep channel activation for residues distal to V282 (A283 and A286).

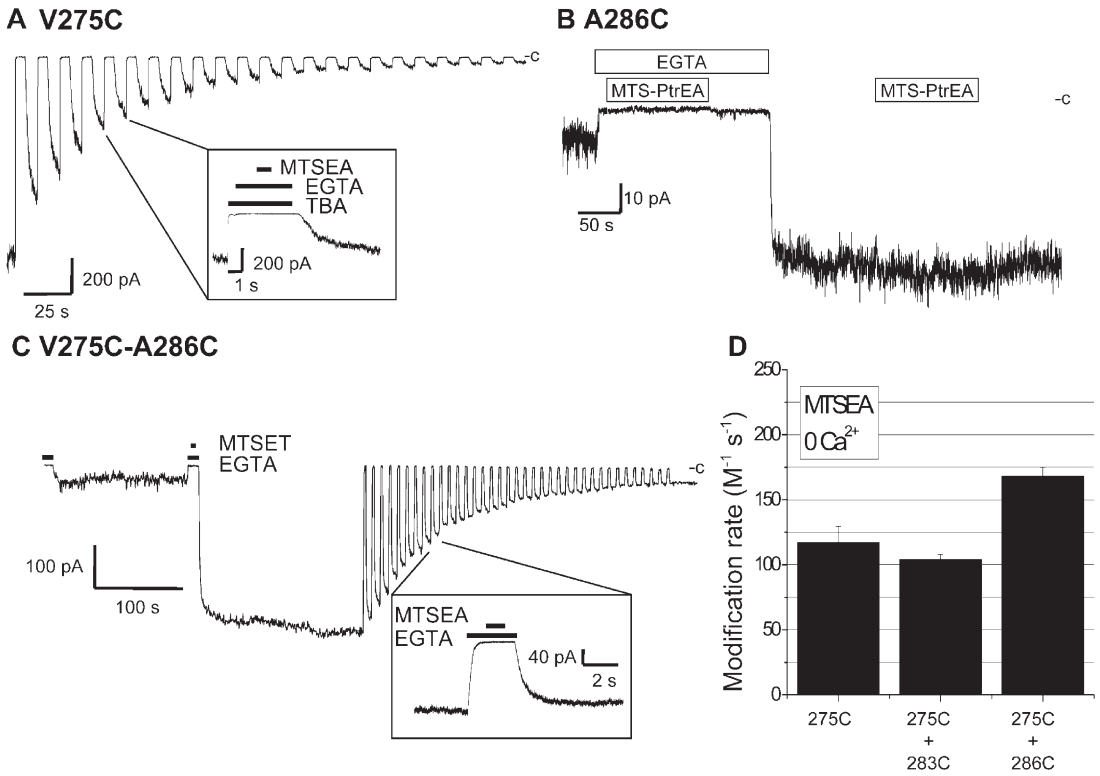

Figure 11. (A) Example of the perfusion protocol implemented to study the effect of TBA on the modification rate by MTSEA of the closed V275C mutant. TBA (1 mM) was first applied during a 0.5-s period prior replacing the Ca^{2+}-containing solution (25 μM) with a zero Ca^{2+} solution containing TBA at the same concentration. MTSEA (5 mM) was applied for 1 s during the zero Ca^{2+} perfusion period. The time course of the current variation induced by MTSEA was assayed according to the procedure described in Fig. 5. Experiments performed at $-Vp = -60$ mV. (B) Modification of the closed (EGTA) A286C mutant by the large MTS reagent MTS-PtrEA. A typical current increase was observed following the internal application of MTS-PtrEA (5 mM) in zero Ca^{2+}, indicating that MTS-PtrEA had access to cysteines at position 286 with KCa3.1 in the closed configuration. A subsequent application of MTS-PtrEA in 25 μM internal Ca^{2+} failed to induce an additional current activation, suggesting that the binding sites were occupied. With dimensions equivalent to a cylinder 12 Å long by 9.5 Å in diameter, the MTS-PtrEA results suggest a pore diameter >9.5 Å, which can hardly be accounted for by a pore structure for the closed KCa3.1 based on the KcsA channel structure. (C) Experimental protocol used to measure the modification rate by MTSEA of cysteines at position 275 in the channel central cavity for the V275C-A286C double mutant channel. An identical protocol was employed to study the V275C-A283C double mutant. MTSET–cysteine complexes were first formed in zero Ca^{2+} conditions (MTSET cannot access the channel cavity under these conditions), and the rate of modification by MTSEA (5 mM) of the cysteines at 275 measured according to the protocol described in Fig. 5. (D) Column graph representation of the modification rates by MTSEA of cysteines at 275 with and without MTSET complexes formed at position 283 and 286, respectively. The modification rates of cysteines at position 275 measured with MTSET–cysteine complexes at position 286 and 283 were estimated at 168 ± 8 $M^{-1}s^{-1}$ ($N = 3$) and 104 ± 12 $M^{-1}s^{-1}$ ($N = 3$), respectively, compared with 112 ± 1 $M^{-1}s^{-1}$ ($N = 7$) for the V275C simple mutant. The presence of charged residues within the alleged channel inner vestibule for the closed KCa3.1 failed to modify the accessibility of MTSEA to cysteine residues located inside the channel central cavity. Taken together these results support a pore structure for the closed KCa3.1 with a large inner vestibule starting at V282.

Second, the pore structure of the closed KCa3.1 channel cannot be accounted for by the inverted teepee-like structure prevailing for the KcsA channel with a constriction at the level of V282 tight enough to be impermeable to molecules such as MTSEA, Et-Hg^+, and Ag^+. Rather, our results support a model where the dimensions of the pore between the cytosolic medium and central cavity for the closed channel range from 4.6 to 5.8 Å in diameter.

Structure of the Closed KCa3.1 Channel and Channel Gating

Our experiments on the closed KCa3.1 showed that the channel modification rates by MTSET were ≈10^3– 10^4 times faster for cysteine residues engineered at positions 283 and 286 compared with cysteines substituting the cavity-lining V275 residues. This effect was strongly size dependent as experiments performed with the smaller MTSEA led to modification rates differing by <20-fold between the A286C and V275C channels. These observations strongly argue for a pore structure of the closed KCa3.1 channel with a constriction located at the level of the T278–A282 residues tight enough to impair the passage of MTSET but leaky to MTSEA. Based on the cross section areas predicted for MTSET and MTSEA it follows that pore diameter for the closed channel between the cytosolic medium and the channel

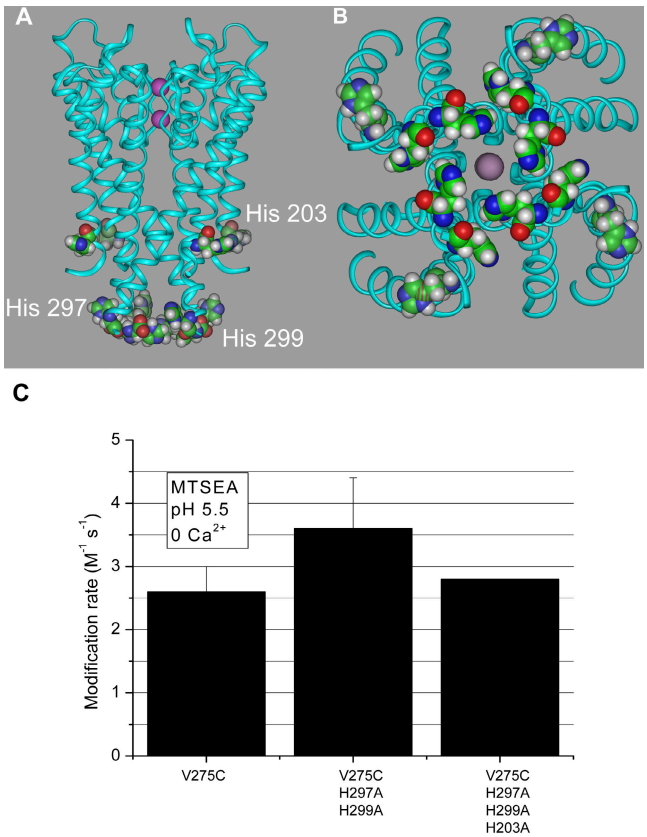

Figure 12. Topology of the closed KCa3.1 channel inner vestibule. (A and B) Side view (A) and view from the cytosolic side (B) of the predicted structure for the closed KCa3.1 derived from KcsA illustrating the presence of a triple histidine ring system surrounding the channel inner vestibule. A double ring of eight histidines at positions 297 and 299 is predicted to be located directly at the pore entrance, whereas four additional histidines on the S5 transmembrane segment should be located at the level of the A286 residues. Because histidine residues are expected to be 90% protonated at pH 5.5, this structure predicts the equivalent of ≈11 positive charges in the channel inner vestibule. Also illustrated are two K^+ ions along the channel pore. (C) Modification rates estimated for the V275C simple mutant and for the triple V275C-H297A-H299A and quadruple V275C-H203A-H297A-H299A mutant channels measured at pH 5.5. The modification rates were estimated by fitting to a single exponential the MTSEA-induced current inhibition for each mutant (K_0). The substitution of the histidine residues by alanine did not alter the MTSEA cysteine accessibility at 275, suggesting that the packing of the TM2 transmembrane segments in KcsA can hardly account for the structure of the closed Kca3.1 channel. Molecular representations were produced with InsightII (Accelry) using the PDB file included as online supplemental material.

cavity should be ranging from 4.6 to 5.8 Å, which is smaller in size than a fully hydrated K^+ ion (6 Å × 6 Å).

These conclusions are also in agreement with our observations that the modification rates of the closed V275C mutant by MTSEA, Et-Hg^+, and Ag^+ were poorly state dependent, in contrast to MTSET, which yielded modification rates at least 10^3-fold slower in zero than in saturating Ca^{2+}. Notably, the modification rates by MTSEA of cysteines at position 282 were nearly identical for the open and closed states, suggesting a minimal structural change at this site in response to channel opening. Although modification rates with Ag^+ could not be estimated for the open V275C mutant, a value of $3 \times 10^7\ s^{-1}M^{-1}$ for the closed state is in agreement with the results reported for the closed/open CNG and Kir2.1 (IRK1J) channels (Flynn and Zagotta, 2003; Xiao et al., 2003) while being 100 times faster than the rates of modification measured in *Shaker* for the residue equivalent to V282 in KCa3.1 (del Camino and Yellen, 2001). In addition, a value of $3.1 \pm 0.6 \times 10^7\ s^{-1}M^{-1}$ is close to the diffusion-limited rate of modification expected for Ag^+, arguing for an unrestricted diffusion of Ag^+ in the channel cavity with V275C in the closed state. Our observations are thus in line with SCAM results reported for the SK2, CNG, and Kir2.1 channels where the helix bundle crossing region was described as being leaky to small sulphydryl reagents such as MTSEA and Ag^+ but not MTSET (Flynn and Zagotta, 2003; Xiao et al., 2003). These authors concluded that the gate controlling K^+ ion flow in ligand-gated channels should be located at the level or close to the selectivity filter. Their results and the observations presented in this work contrast with the findings reported on the voltage-gated *Shaker* channel where a huge decrease in the accessibility of the residues above the bundle crossing (V474 corresponding to V282 in KCa3.1, see Fig. 1 B) was measured with MTSET, MTSEA, and Ag^+ when the channel was in a closed configuration (Liu et al., 1997; del Camino and Yellen, 2001). The structural changes involved in the opening of the pore thus appear to differ considerably between KCa3.1 and voltage-gated channels such as *Shaker*.

Can MTSEA Be Trapped in the Channel Cavity?

Because the MTSEA results set the lower limit of the pore diameter for the closed channel to 4.6 Å, which is nearly two times larger than the van der Walls diameter (2.6 Å) of a K^+ ion but less than the diameter of a fully hydrated K^+ (6 Å), alternative interpretations for the weak state dependence observed with the V275C mutant need to be considered. One of these interpretations refers to the trapping of MTSEA inside the channel cavity (Phillips et al., 2003). The kinetic scheme related to MTSEA trapping can be expressed as (see Phillips et al., 2003)

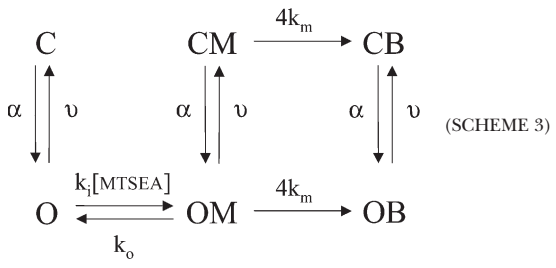

where α and υ correspond to the average channel opening and closing rates, OM and CM the kinetic states associated to the open and closed channel configurations with MTSEA in the binding site, and CB, OB the state following the irreversible binding of MTSEA to the target cysteines. We found from single channel recordings that the mean open time of the V275C mutant is of the order of 16 ms and varies little as a function of the internal Ca^{2+} concentration (unpublished data). This observation sets the upper limit for the closing rate υ to 63 s^{-1}. In addition, the results presented in Fig. 9 indicate that the reaction rate, k_m, for the open V275C mutant is approximately equal to 7 s^{-1} with $[MTSAE]_{1/2} \approx 35$ mM, and our pH analysis showed that in the closed configuration the MTSEA entry rate for the V275C mutant corresponds to $k_i \approx 480\ M^{-1}s^{-1}$. This value constitutes a lower limit, the entry rate being expected to be higher for the open channel configuration. With k_i set to 10^4 $M^{-1}s^{-1}$ and $k_m = 7\ s^{-1}$, the expression derived for $[MTS]_{1/2}$ (Appendix, Eq. A5) predicts an exit rate $k_o \approx 320\ s^{-1}$. The variation in modification rate as a function of the channel open probability can be estimated by solving the kinetic scheme 3 numerically with υ set to 63 s^{-1}. This analysis led to the conclusion that a trapping mechanism would require an open probability $Po > 0.05$ to account for a measured inhibition rate of 0.1 s^{-1} in zero Ca^{2+} for 1 mM MTSEA. An identical result was obtained assuming an entry rate $k_i = 10^5\ M^{-1}s^{-1}$. If k_i is presumed to be the same for the open and closed state ($k_i \approx 480\ M^{-1}s^{-1}$), a $Po > 0.1$ would then be required to account for our results. A *Po* of 0.05 corresponds to the level of channel activity expected for a 0.6 μM internal Ca^{2+} solution, which is at least 50 times higher than the expected Ca^{2+} concentration in our EGTA-buffered Ca^{2+}-free solutions (Simoes et al., 2002). A smaller *Po* of 0.02 would however be required if the mean open time of the V275C mutant is set to 0.1 or 1 ms with $k_i > 10^4\ M^{-1}s^{-1}$. This level of channel activity still corresponds to an internal Ca^{2+} concentration of 0.5 μM, arguing also against a trapping mechanism. Finally, *Po* ranging from 0.02 to 0.1 in the absence of Ca^{2+} would have resulted in current level for the V275C mutant clearly distinct from the current level after MTSEA block. Such a behavior was not observed experimentally. The absence of state-dependent modifications by MTSEA of the V275C mutant is not likely therefore to be accountable by a trapping mechanism.

An alternative explanation to the observation that MTSEA has access from the cytoplasmic side to the channel cavity with KCa3.1 in a closed configuration would be that MTSEA uses a diffusion pathway not applicable to K^+ ions and/or diffuses through the channel pore in a deprotonated form. Evidence arguing against this interpretation comes from the TBA protection experiments and from the pH dependence of the 275C modification rate by MTSEA, which support a mechanism where MTSEA accesses the channel central cavity from the cytosolic medium as a protonated cation. Our MTSEA results are thus compatible with a model where the weak state dependence of the 275C modification rate by MTSEA is likely to reflect a pore structure for the closed KCa3.1 with a pore constriction tight enough to impair the passage of MTSET but leaky to smaller reagents such as MTSEA, Ag^+, and Et-Hg^+.

Toward a 3D Representation of the Closed KCa3.1 Channel Structure

The results on the 275C accessibility to MTSEA in zero Ca^{2+} also need to be interpreted in light of our findings on the dimensions of the closed KCa3.1 inner vestibule. Our results show for instance that the large MTS-PtrEA had access to the 286C residue in zero Ca^{2+}. Because a MTS-PtrEA molecule fits into a cylinder 9.5 Å diameter and 12 Å long, the functional pore dimensions for the closed channel below A286 should be >9.5 Å comparatively to 4.2 Å as predicted on the basis of a KcsA-like structure. Furthermore, the addition of positively charged MTSET–cysteine complexes at position 283 did not impair MTSEA from diffusing inside the channel cavity in the closed configuration. With a predicted pore diameter of 6.2 Å at A283, a KcsA-based representation of the closed KCa3.1 can hardly account for these observations. Taken together, our analysis does not support a model for the closed KCa3.1 channel where the cytoplasmic pore structure would be represented by an inverted tepee-like structure as described for KcsA. In accordance with this proposal, the neutralization at pH 5.5 of 11 equivalent positive charges in the V275C-H203A-H297A-H299A mutant did not alter the modification rates by MTSEA of the cysteines at 275. This observation would be compatible with a model where the residues distal to V282 residues are connected to rather wide internal vestibule. Alternatively, the secondary structure of the S6 segment distal to 283 may not be totally represented by an α helix as predicted on the basis of a KcsA structure but may contain some turn/coil regions as observed with MthK channel, so that the residues predicted to be facing the channel pore may be oriented in another direction. This could explain the inefficiency of the MTSET–cysteine complexes at 283 to impair the access of MTSEA to the channel cavity with the channel closed.

Gating of KCa3.1 Channel, a Multilocation Process

The extent of the contribution of the bundle crossing region to the ligand-dependent gating of ion channels is not fully established. Recent results obtained with the pH-dependent KcsA and Ca^{2+}-activated MthK channels argue for a multiple gate system where the stimulus-dependent gate at bundle crossing would be determinant to the duration of individual opening channel bursts with intraburst fluctuations governed by a second gating

process located at the level of the selectivity filter or close to it (Cordero-Morales et al., 2006; Zadek and Nimigean, 2006). A recent study where the opening of the bundle crossing in KcsA was monitored using a fluorescence-based approach also concluded in the presence of a second gate at the level of the selectivity filter (Blunck et al., 2006). The finding that the accessibility of cysteine residues at position 275 was poorly state dependent when MTSEA, Et-Hg^+, and Ag^+ were used as sulphydryl reagents does not favor a model where the constriction region from V282 to A286 would act as an activation gate. This conclusion is in accordance with our results demonstrating that the closed KCa3.1 cannot be represented by a KcsA-like structure. The possibility that the selectivity filter region contributes to the activation of ligand-gated channels has been discussed in several studies (Bruening-Wright et al., 2002) and a similar mechanism could prevail in KCa3.1. The S6 segments would then act as transducers conveying the structural changes from the bundle crossing to the selectivity filter. Our results demonstrate nevertheless that the action of Ca^{2+} on KCa3.1 is consistent with an opening of the pore at the C-terminal end of S6. This conclusion is mainly supported by the observation that the accessibility of the cysteines at 275 to MTSET is state dependent. It remains to be determined to what extent an increase in pore dimensions corresponding at least to the diameter of an MTSET molecule (5.8 Å) or larger is essential for channel gating. Opening of the pore in the C terminus of S6 may serve other functions such as to modify the geometry of the cavity and/or the selectivity filter region for gating, or favor the diffusion of K^+ ions through the V282 constriction region thus increasing the channel conductance (Li and Aldrich, 2006). The observation that MTSEA and MTSET could activate the A283C and A286C mutants also raises the possibility of a contribution of the S6 segment from A283 to A286 to channel gating distinct from a gating process involving the selectivity filter and/or the cavity region. Several single channel analyses have already demonstrated that the KCa3.1 channel open probability is smaller than one at saturating internal Ca^{2+} concentrations, with typical values of 0.2–0.4 (Sauvé et al., 1986; Keen et al., 1999). The fact that MTSET and MTSEA acting on A283C or A286C caused an increase of the channel maximum open probability at saturating Ca^{2+} therefore suggests additional gating mechanisms that are distinct from a Ca^{2+}-dependent opening of the channel pore at the C-terminal end of S6. These possibilities need further investigations.

Conclusions

Our results do not support a KcsA-like structure for the pore region of the closed KCa3.1 channel. It is therefore unlikely that a constriction at the C-terminal end of S6 contributes to the gating process of KCa3.1 by Ca^{2+}. Our results point nevertheless toward a pore structure with a diameter d such that 4.6 Å $<$ d $<$ 5.8 Å connecting the channel central cavity and a wide cytoplasmic vestibule.

APPENDIX

The time course of cysteine modification predicted from the kinetic Scheme 1 presented in Materials and methods is given by

$$S_B(n,t) = 1 + \frac{1}{K_s - K_n}\left[K_n e^{-K_s t} - K_1 e^{-K_n t}\right] \quad \text{(A1)}$$

where

$$K_n + K_s = k_i f_n^i [MTS] + k_o f_n^o + (4-n)k_m \quad \text{(A2)}$$

and

$$K_n K_s = (4-n)k_i f_n^i [MTS] k_m \quad \text{(A3)}$$

In conditions where $K_s >> K_n$, the expression (A1) reduces to

$$S_B(n,t) = 1 - e^{-K_n t} \quad \text{(A4)}$$

with K_n now expressed as

$$K_n \cong \frac{(4-n)k_i f_n^i [MTS] k_m}{k_i f_n^i [MTS] + k_o f_n^o + (4-n)k_m} \quad \text{(A5)}$$

Eq. A5 corresponds to a standard Michaelis Mentel equation with a maximum modification rate given by $(4-n)k_m$ and a [MTS] concentration for half maximum rate ($[MTS]_{1/2}$) equal to $(k_o f_n^o + (4-n)k_m)/k_i f_n^i$. In low [MTS] concentrations Eq. A5 reduces to

$$K_n \cong \frac{(4-n)k_i f_n^i k_m}{k_o f_n^o + (4-n)k_m}[MTS] \quad \text{(A6)}$$

so that K_n is now a linear function of [MTS] with a slope given by $(4-n)k_m k_i f_n^i / (k_o f_n^o + (4-n)k_m)$. In conditions where $k_m << k_o$, Eq. A6 can be expressed as

$$K_n \cong \frac{(4-n)k_i f_n^i k_m}{k_o f_n^0}[MTS] \quad \text{(A7)}$$

The modification rate per cysteine K_C in the kinetic Model I presented in Materials and methods thus formally corresponds to $K_C = k_m k_i / k_o$ with $f_n = f_n^i / f_n^o$. In contrast, when the reaction rate with the cysteine is considered much faster than the entry and exit rates k_i and k_o ($k_m >> k_o + k_i$[MTS]) the rates of transition read $K_n = k_i f_n^i [MTS]$ so that the binding of MTS reagents to a channel has now to be modeled according to the scheme presented in Model II with $K_n = k_i$[MTS] = constant assuming $f_n^i = 1$. The modification rates

estimated under these conditions truly reflect the accessibility of the MTS reagent to the cysteine binding site. Such condition may not however always prevail, so the modification rates measured experimentally cannot be systematically interpreted as a measurement of the MTS accessibility to a target cysteine residue.

We thank Drs. Daniel Devor and Benoit Roux for stimulating discussions. We also acknowledge the work of Ms. Julie Verner for expert oocyte preparation.

This work was supported by grants from the Canadian Institutes of Health Research (MOP 7769), from the Canadian Heart and Stroke Foundation, and from the Canadian Cystic Fibrosis Foundation.

Olaf S. Andersen served as editor.

Submitted: 21 December 2006
Accepted: 22 February 2007

REFERENCES

Banderali, U., H. Klein, L. Garneau, M. Simoes, L. Parent, and R. Sauvé. 2004. New insights on the voltage dependence of the KCa3.1 channel block by internal TBA. *J. Gen. Physiol.* 124:333–348.

Blunck, R., J.F. Cordero-Morales, L.G. Cuello, E. Perozo, and F. Bezanilla. 2006. Detection of the opening of the bundle crossing in KcsA with fluorescence lifetime spectroscopy reveals the existence of two gates for ion conduction. *J. Gen. Physiol.* 128:569–581.

Bruening-Wright, A., M.A. Schumacher, J.P. Adelman, and J. Maylie. 2002. Localization of the activation gate for small conductance Ca^{2+}-activated K^+ channels. *J. Neurosci.* 22:6499–6506.

Cordero-Morales, J.F., L.G. Cuello, Y. Zhao, V. Jogini, D.M. Cortes, B. Roux, and E. Perozo. 2006. Molecular determinants of gating at the potassium-channel selectivity filter. *Nat. Struct. Mol. Biol.* 13:311–318.

del Camino, D., and G. Yellen. 2001. Tight steric closure at the intracellular activation gate of a voltage-gated K^+ channel. *Neuron.* 32:649–656.

Doyle, D.A., J.M. Cabral, R.A. Pfuetzner, A. Kuo, J.M. Gulbis, S.L. Cohen, B.T. Chait, and R. MacKinnon. 1998. The structure of the potassium channel: molecular basis of K^+ conduction and selectivity. *Science.* 280:69–77.

Flynn, G.E., and W.N. Zagotta. 2003. A cysteine scan of the inner vestibule of cyclic nucleotide-gated channels reveals architecture and rearrangement of the pore. *J. Gen. Physiol.* 121:563–582.

Holmgren, M., Y. Liu, Y. Xu, and G. Yellen. 1996. On the use of thiol-modifying agents to determine channel topology. *Neuropharmacology.* 35:797–804.

Joiner, W.J., R. Khanna, L.C. Schlichter, and L.K. Kaczmarek. 2001. Calmodulin regulates assembly and trafficking of SK4/IK1 Ca^{2+}-activated K^+ channels. *J. Biol. Chem.* 276:37980–37985.

Karlin, A., and M.H. Akabas. 1998. Substituted-cysteine accessibility method. *Methods Enzymol.* 293:123–145.

Keen, J.E., R. Khawaled, D.L. Farrens, T. Neelands, A. Rivard, C.T. Bond, A. Janowsky, B. Fakler, J.P. Adelman, and J. Maylie. 1999. Domains responsible for constitutive and Ca^{2+}-dependent interactions between calmodulin and small conductance Ca^{2+}-activated potassium channels. *J. Neurosci.* 19:8830–8838.

Khanna, R., M.C. Chang, W.J. Joiner, L.K. Kaczmarek, and L.C. Schlichter. 1999. hSK4/hIK1, a calmodulin-binding KCa channel in human T lymphocytes. Roles in proliferation and volume regulation. *J. Biol. Chem.* 274:14838–14849.

Kohler, M., B. Hirschberg, C.T. Bond, J.M. Kinzie, N.V. Marrion, J. Maylie, and J.P. Adelman. 1996. Small-conductance, calcium-activated potassium channels from mammalian brain. *Science.* 273:1709–1714.

Laskowski, R.A., M.W. MacArthur, D.S. Moss, and J.M. Thornton. 1993. PROCHECK: a program to check the stereochemical quality of protein structures. *J. Appl. Crys.* 26:283–291.

Lee, W.S., T.J. Ngo-Anh, A. Bruening-Wright, J. Maylie, and J.P. Adelman. 2003. Small conductance Ca^{2+}-activated K^+ channels and calmodulin: cell surface expression and gating. *J. Biol. Chem.* 278:25940–25946.

LeMasurier, M., L. Heginbotham, and C. Miller. 2001. KcsA: it's a potassium channel. *J. Gen. Physiol.* 118:303–314.

Li, W., and R.W. Aldrich. 2006. State-dependent block of BK channels by synthesized Shaker ball peptides. *J. Gen. Physiol.* 128:423–441.

Liu, Y., M. Holmgren, M.E. Jurman, and G. Yellen. 1997. Gated access to the pore of a voltage-dependent K^+ channel. *Neuron.* 19:175–184.

Pascual, J.M., and A. Karlin. 1998. State-dependent accessibility and electrostatic potential in the channel of the acetylcholine receptor. Inferences from rates of reaction of thiosulfonates with substituted cysteines in the M2 segment of the α subunit. *J. Gen. Physiol.* 111:717–739.

Pedersen, K.A., N.K. Jorgensen, B.S. Jensen, and S.P. Olesen. 2000. Inhibition of the human intermediate-conductance, Ca^{2+}-activated K^+ channel by intracellular acidification. *Pflugers Arch.* 440:153–156.

Phillips, L.R., D. Enkvetchakul, and C.G. Nichols. 2003. Gating dependence of inner pore access in inward rectifier K^+ channels. *Neuron.* 37:953–962.

Rittenhouse, A.R., D.H. Vandorpe, C. Brugnara, and S.L. Alper. 1997. The antifungal imidazole clotrimazole and its major in vivo metabolite are potent blockers of the calcium-activated channel in murine erythroleukemia cells. *J. Membr. Biol.* 157:177–191.

Sali, A., and T.L. Blundell. 1993. Comparative protein modelling by satisfaction of spatial restraints. *J. Mol. Biol.* 234:779–815.

Sauvé, R., C. Simoneau, R. Monette, and G. Roy. 1986. Single-channel analysis of the potassium permeability in HeLa cancer cells: evidence for a calcium-activated potassium channel of small unitary conductance. *J. Membr. Biol.* 92:269–282.

Simoes, M., L. Garneau, H. Klein, U. Banderali, F. Hobeila, B. Roux, L. Parent, and R. Sauve. 2002. Cysteine mutagenesis and computer modeling of the S6 region of an intermediate conductance IKCa channel. *J. Gen. Physiol.* 120:99–116.

Stocker, M. 2004. Ca^{2+}-activated K^+ channels: molecular determinants and function of the SK family. *Nat. Rev. Neurosci.* 5:758–770.

Vergara, C., R. Latorre, N.V. Marrion, and J.P. Adelman. 1998. Calcium-activated potassium channel. *Curr. Opin. Neurobiol.* 8:321–329.

Wallner, B., and A. Elofsson. 2003. Can correct protein models be identified? *Protein Sci.* 12:1073–1086.

Wilson, G.G., and A. Karlin. 1998. The location of the gate in the acetylcholine receptor channel. *Neuron.* 20:1269–1281.

Wulff, H., G.A. Gutman, M.D. Cahalan, and K.G. Chandy. 2001. Delineation of the clotrimazole/TRAM-34 binding site on the intermediate conductance calcium-activated potassium channel, IKCa1. *J. Biol. Chem.* 276:32040–32045.

Xiao, J., X.G. Zhen, and J. Yang. 2003. Localization of PIP2 activation gate in inward rectifier K^+ channels. *Nat. Neurosci.* 6:811–818.

Zadek, B., and C.M. Nimigean. 2006. Calcium-dependent gating of MthK, a prokaryotic potassium channel. *J. Gen. Physiol.* 127:673–685.